

AD-A041 917

OAKLAND UNIV ROCHESTER MICH SCHOOL OF ENGINEERING  
DIRECT DETERMINATION OF FLEXURAL STRAINS IN PLATES USING PROJEC--ETC(U)  
JUN 77 C Y LIANG, Y Y HUNG, A J DURELLI

F/G 20/11

N00014-76-C-0487

NL

UNCLASSIFIED

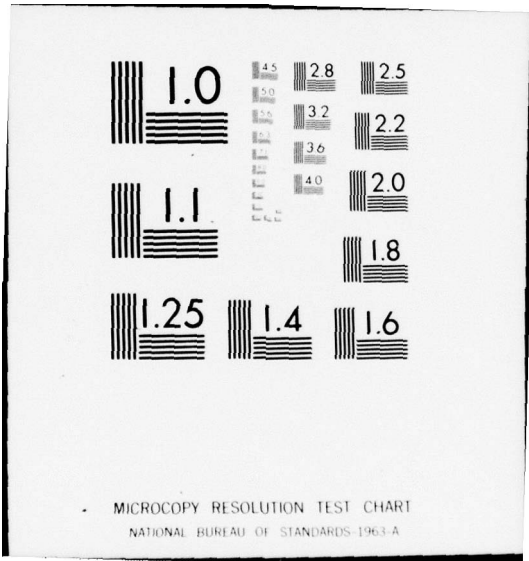
45

| OF |  
ADA041917



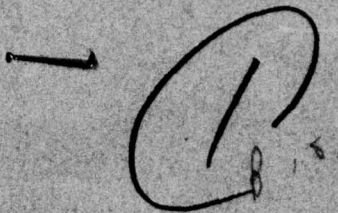
END

DATE  
FILMED  
8 - 77



MICROCOPY RESOLUTION TEST CHART  
NATIONAL BUREAU OF STANDARDS-1963-A

AD A041917



DIRECT DETERMINATION OF FLEXURAL  
STRAINS IN PLATES USING PROJECTED GRATINGS

BY

C. Y. LIANG, Y. Y. HUNG, A. J. DURELLI AND J. D. HOVANESIAN

SPONSORED BY

OFFICE OF NAVAL RESEARCH  
DEPARTMENT OF THE NAVY  
WASHINGTON, D.C. 20025

ON

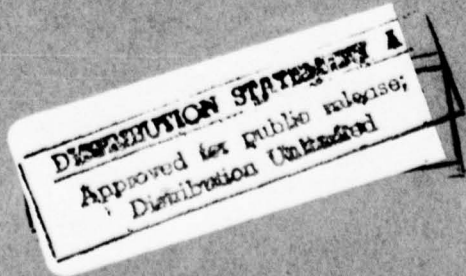
CONTRACT No. N00014-76-C-0487  
O.U. PROJECT No. 30339-49  
REPORT No. 45



SCHOOL OF ENGINEERING  
OAKLAND UNIVERSITY  
ROCHESTER, MICHIGAN 48063

JUNE 1977

AD No. \_\_\_\_\_  
DDC FILE COPY



6

DIRECT DETERMINATION OF FLEXURAL STRAINS IN PLATES USING PROJECTED GRATINGS

by

10

C. Y. Liang, Y. Y. Hung, A. J. Durelli and J. D. Hovanesian

Sponsored by

Office of Naval Research  
Department of the Navy  
Washington, D.C. 20025

15 on

Contract No. N00014-76-C-0487  
O.U. Project No. 30339-49  
Report No. 45

25/ LPN

14



School of Engineering  
Oakland University  
Rochester, Michigan 48063

12 29 p.

11

June 1977

ACCESSION NO.	
NTIS	White Section <input checked="" type="checkbox"/>
DIC	Buff Section <input type="checkbox"/>
UNANNOUNCED	<input type="checkbox"/>
JUSTIFICATION	
BY	
DISTRIBUTION AVAILABILITY CODES	
DIS.	AVAIL. and/or SPECIAL
A	

1472  
405 252

LB

DIRECT DETERMINATION OF FLEXURAL  
STRAINS IN PLATES USING PROJECTED GRATINGS

by

C. Y. Liang, Y. Y. Hung, A. J. Durelli, J. D. Hovanesian

Abstract

It is proposed in this paper to use projected gratings to determine principal strains in plates subjected to bending. The method requires the rotation of one photograph of the deformed grating over a copy of itself, the rotation taking place about the point at which the bending strains are desired. The idea previously suggested by Stetson to double differentiate holograms of bent plates has been extended and verified with an application to a plate subjected to twisting. The proposed method is easy to use and permits the determination of principal strains in plates subjected to much larger deflections than the ones that can be studied using holograms. Suggestions to improve the precision of the determination are also made.

Previous Technical Reports to the Office of Naval Research

1. A. J. Durelli, "Development of Experimental Stress Analysis Methods to Determine Stresses and Strains in Solid Propellant Grains"--June 1962. Developments in the manufacturing of grain-propellant models are reported. Two methods are given: a) cementing routed layers and b) casting.
2. A. J. Durelli and V. J. Parks, "New Method to Determine Restrained Shrinkage Stresses in Propellant Grain Models"--October 1962. The birefringence exhibited in the curing process of a partially restrained polyurethane rubber is used to determine the stress associated with restrained shrinkage in models of solid propellant grains partially bonded to the case.
3. A. J. Durelli, "Recent Advances in the Application of Photoelasticity in the Missile Industry"--October 1962. Two- and three-dimensional photoelastic analysis of grains loaded by pressure and by temperature are presented. Some applications to the optimization of fillet contours and to the redesign of case joints are also included.
4. A. J. Durelli and V. J. Parks, "Experimental Solution of Some Mixed Boundary Value Problems"--April 1964. Means of applying known displacements and known stresses to the boundaries of models used in experimental stress analysis are given. The application of some of these methods to the analysis of stresses in the field of solid propellant grains is illustrated. The presence of the "pinching effect" is discussed.
5. A. J. Durelli, "Brief Review of the State of the Art and Expected Advance in Experimental Stress and Strain Analysis of Solid Propellant Grains"--April 1964. A brief review is made of the state of the experimental stress and strain analysis of solid propellant grains. A discussion of the prospects for the next fifteen years is added.
6. A. J. Durelli, "Experimental Strain and Stress Analysis of Solid Propellant Rocket Motors"--March 1965. A review is made of the experimental methods used to strain-analyze solid propellant rocket motor shells and grains when subjected to different loading conditions. Methods directed at the determination of strains in actual rockets are included.
7. L. Ferrer, V. J. Parks and A. J. Durelli, "An Experimental Method to Analyze Gravitational Stresses in Two-Dimensional Problems"--October 1965. Photoelasticity and moiré methods are used to solve two-dimensional problems in which gravity-stresses are present.

8. A. J. Durelli, V. J. Parks and C. J. del Rio, "Stresses in a Square Slab Bonded on One Face to a Rigid Plate and Shrunk"--November 1965.  
A square epoxy slab was bonded to a rigid plate on one of its faces in the process of curing. In the same process the photoelastic effects associated with a state of restrained shrinkage were "frozen-in." Three-dimensional photoelasticity was used in the analysis.
9. A. J. Durelli, V. J. Parks and C. J. del Rio, "Experimental Determination of Stresses and Displacements in Thick-Wall Cylinders of Complicated Shape"--April 1966.  
Photoelasticity and moiré are used to analyze a three-dimensional rocket shape with a star shaped core subjected to internal pressure.
10. V. J. Parks, A. J. Durelli and L. Ferrer, "Gravitational Stresses Determined Using Immersion Techniques"--July 1966.  
The methods presented in Technical Report No. 7 above are extended to three-dimensions. Immersion is used to increase response.
11. A. J. Durelli and V. J. Parks. "Experimental Stress Analysis of Loaded Boundaries in Two-Dimensional Second Boundary Value Problems"--February 1967.  
The pinching effect that occurs in two-dimensional bonding problems, noted in Reports 2 and 4 above, is analyzed in some detail.
12. A. J. Durelli, V. J. Parks, H. C. Feng and F. Chiang, "Strains and Stresses in Matrices with Inserts,"-- May 1967.  
Stresses and strains along the interfaces, and near the fiber ends, for different fiber end configurations, are studied in detail.
13. A. J. Durelli, V. J. Parks and S. Uribe, "Optimization of a Slot End Configuration in a Finite Plate Subjected to Uniformly Distributed Load,"--June 1967.  
Two-dimensional photoelasticity was used to study various elliptical ends to a slot, and determine which would give the lowest stress concentration for a load normal to the slot length.
14. A. J. Durelli, V. J. Parks and Han-Chow Lee, "Stresses in a Split Cylinder Bonded to a Case and Subjected to Restrained Shrinkage,"--January 1968.  
A three-dimensional photoelastic study that describes a method and shows results for the stresses on the free boundaries and at the bonded interface of a solid propellant rocket.
15. A. J. Durelli, "Experimental Stress Analysis Activities in Selected European Laboratories"--August 1968.  
This report has been written following a trip conducted by the author through several European countries. A list is given of many of the laboratories doing important experimental stress analysis work and of the people interested in this kind of work. An attempt has been made to abstract the main characteristics of the methods used in some of the countries visited.

16. V. J. Parks, A. J. Durelli and L. Ferrer, "Constant Acceleration Stresses in a Composite Body"--October 1968.  
Use of the immersion analogy to determine gravitational stresses in two-dimensional bodies made of materials with different properties.
17. A. J. Durelli, J. A. Clark and A. Kochev, "Experimental Analysis of High Frequency Stress Waves in a Ring"--October 1968.  
A method for the complete experimental determination of dynamic stress distributions in a ring is demonstrated. Photoelastic data is supplemented by measurements with a capacitance gage used as a dynamic lateral extensometer.
18. J. A. Clark and A. J. Durelli, "A Modified Method of Holographic Interferometry for Static and Dynamic Photoelasticity"--April 1968.  
A simplified absolute retardation approach to photoelastic analysis is described. Dynamic isopachics are presented.
19. J. A. Clark and A. J. Durelli, "Photoelastic Analysis of Flexural Waves in a Bar"--May 1969.  
A complete direct, full-field optical determination of dynamic stress distribution is illustrated. The method is applied to the study of flexural waves propagating in a urethane rubber bar. Results are compared with approximate theories of flexural waves.
20. J. A. Clark and A. J. Durelli, "Optical Analysis of Vibrations in Continuous Media"--June 1969.  
Optical methods of vibration analysis are described which are independent of assumptions associated with theories of wave propagation. Methods are illustrated with studies of transverse waves in prestressed bars, snap loading of bars and motion of a fluid surrounding a vibrating bar.
21. V. J. Parks, A. J. Durelli, K. Chandrashekhara and T. L. Chen, "Stress Distribution Around a Circular Bar, with Flat and Spherical Ends, Embedded in a Matrix in a Triaxial Stress Field"--July 1969.  
A Three-dimensional photoelastic method to determine stresses in composite materials is applied to this basic shape. The analyses of models with different loads are combined to obtain stresses for the triaxial cases.
22. A. J. Durelli, V. J. Parks and L. Ferrer, "Stresses in Solid and Hollow Spheres Subjected to Gravity or to Normal Surface Traction"--October 1969.  
The method described in Report No. 10 above is applied to two specific problems. An approach is suggested to extend the solutions to a class of surface traction problems.
23. J. A. Clark and A. J. Durelli, "Separation of Additive and Subtractive Moiré Patterns"--December 1969.  
A spatial filtering technique for adding and subtracting images of several gratings is described and employed to determine the whole field of Cartesian shears and rigid rotations.

24. R. J. Sanford and A. J. Durelli, "Interpretation of Fringes in Stress-Holo-Interferometry"--July 1970.  
Errors associated with interpreting stress-holo-interferometry patterns as the superposition of isopachics (with half order fringe shifts) and isochromatics are analyzed theoretically and illustrated with computer generated holographic interference patterns.
25. J. A. Clark, A. J. Durelli and P. A. Laura, "On the Effect of Initial Stress on the Propagation of Flexural Waves in Elastic Rectangular Bars"--December 1970.  
Experimental analysis of the propagation of flexural waves in prismatic, elastic bars with and without prestressing. The effects of prestressing by axial tension, axial compression and pure bending are illustrated.
26. A. J. Durelli and J. A. Clark, "Experimental Analysis of Stresses in a Buoy-Cable System Using a Birefringent Fluid"--February 1971.  
An extension of the method of photoviscous analysis is presented which permits quantitative studies of strains associated with steady state vibrations of immersed structures. The method is applied in an investigation of one form of behavior of buoy-cable systems loaded by the action of surface waves.
27. A. J. Durelli and T. L. Chen, "Displacements and Finite-Strain Fields in a Sphere Subjected to Large Deformations"--February 1972.  
Displacements and strains (ranging from 0.001 to 0.50) are determined in a polyurethane sphere subjected to several levels of diametral compression. A 500 lines-per-inch grating was embedded in a meridian plane of the sphere and moiré effect produced with a non-deformed master. The maximum applied vertical displacement reduced the diameter of the sphere by 27 per cent.
28. A. J. Durelli and S. Machida, "Stresses and Strain in a Disk with Variable Modulus of Elasticity"--March 1972.  
A transparent material with variable modulus of elasticity has been manufactured that exhibits good photoelastic properties and can also be strain analyzed by moiré. The results obtained suggests that the stress distribution in the homogeneous disk. It also indicates that the strain fields in both cases are very different, but that it is possible, approximately, to obtain the stress field from the strain field using the value of  $E$  at every point, and Hooke's law.
29. A. J. Durelli and J. Buitrago, "State of Stress and Strain in A Rectangular Belt Pulled Over a Cylindrical Pulley"--June 1972.  
Two- and three-dimensional photoelasticity as well as electrical strain gages, dial gages and micrometers are used to determine the stress distribution in a belt-pulley system. Contact and tangential stress for various contact angles and friction coefficients are given.

30. T. L. Chen and A. J. Durelli, "Stress Field in a Sphere Subjected to Large Deformations"--June 1972.  
Strain fields obtained in a sphere subjected to large diametral compressions from a previous paper were converted into stress fields using two approaches. First, the concept of strain-energy function for an isotropic elastic body was used. Then the stress field was determined with the Hookean type natural stress-natural strain relation. The results so obtained were also compared.
31. A. J. Durelli, V. J. Parks and H. M. Hasseem, "Helices Under Load"--July 1973.  
Previous solutions for the case of close coiled helical springs and for helices made of thin bars are extended. The complete solution is presented in graphs for the use of designers. The theoretical development is correlated with experiments.
32. T. L. Chen and A. J. Durelli, "Displacements and Finite Strain Fields in a Hollow Sphere Subjected to Large Elastic Deformations"--September 1973.  
The same methods described in No. 27, were applied to a hollow sphere with an inner diameter one half the outer diameter. The hollow sphere was loaded up to a strain of 30 per cent on the meridian plane and a reduction of the diameter by 20 per cent.
33. A. J. Durelli, H. H. Hasseem and V. J. Parks, "New Experimental Method in Three-Dimensional Elastostatics"--December 1973.  
A new material is reported which is unique among three-dimensional stress-freezing materials, in that, in its heated (or rubbery) state it has a Poisson's ratio which is appreciably lower than 0.5. For a loaded model, made of this material, the unique property allows the direct determination of stresses from strain measurements taken at interior points in the model.
34. J. Wolak and V. J. Parks, "Evaluation of Large Strains in Industrial Applications"--April 1974.  
It was shown that Mohr's circle permits the transformation of strain from one axis of reference to another, irrespective of the magnitude of the strain, and leads to the evaluation of the principal strain components from the measurement of direct strain in three directions.
35. A. J. Durelli, "Experimental Stress Analysis Activities in Selected European Laboratories"--April 1975.  
Continuation of Report No. 15 after a visit to Belgium, Holland, Germany, France, Turkey, England and Scotland.
36. A. J. Durelli, V. J. Parks and J. O. Bühler-Vidal, "Linear and Non-linear Elastic and Plastic Strains in a Plate with a Big Hole Loaded Axially in its Plane"--July 1975.  
Strain analysis of the ligament of a plate with a big hole indicates that both geometric and material non-linearity may take place. The strain concentration factor was found to vary from 1 to 2 depending on the level of deformation.

37. A. J. Durelli, V. Pavlin, J. O. Bühler-Vidal and G. Ome, "Elastostatics of a Cubic Box Subjected to Concentrated Loads"--August 1975.  
Analysis of experimental strain, stress and deflection of a cubic box subjected to concentrated loads applied at the center of two opposite faces. The ratio between the inside span and the wall thickness was varied between approximately 5 and 121.
38. A. J. Durelli, V. J. Parks and J. O. Bühler-Vidal, "Elastostatics of Cubic Boxes Subjected to Pressure"--March 1976.  
Experimental analysis of strain, stress and deflections in a cubic box subjected to either internal or external pressure. Inside span-to-wall thickness ratio varied from 5 to 14.
39. Y. Y. Hung, J. D. Hovanesian and A. J. Durelli, "New Optical Method to Determine Vibration-Induced Strains with Variable Sensitivity After Recording"--November 1976.  
A steady state vibrating object is illuminated with coherent light and its image slightly misfocused. The resulting specklegram is "time-integrated" as when Fourier filtered gives derivatives of the vibrational amplitude.
40. Y. Y. Hung, C. Y. Liang, J. D. Hovanesian and A. J. Durelli, "Cyclic Stress Studies by Time-Averaged Photoelasticity"--November 1976.  
"Time-averaged isochromatics" are formed when the photographic film is exposed for more than one period. Fringes represent amplitudes of the oscillating stress according to the zeroth order Bessel function.
41. Y. Y. Hung, C. Y. Liang, J. D. Hovanesian and A. J. Durelli, "Time-Averaged Shadow Moiré Method for Studying Vibrations"--November 1976.  
Time-averaged shadow moiré permits the determination of the amplitude distribution of the deflection of a steady vibrating plate.
42. J. Buitrago and A. J. Durelli, "On the Interpretation of Shadow-Moiré Fringes"--April 1977.  
Possible rotations and translations of the grating are considered in a general expression to interpret shadow-moiré fringes and on the sensitivity of the method. Application to an inverted perforated tube.
43. J. der Hovanesian, "18th Polish Solid Mechanics Conference." Published in European Scientific Notes of the Office of Naval Research, in London, England, Dec. 31, 1976.  
Comments on the planning and organization of, and scientific content of paper presented at the 18th Polish Solid Mechanics Conference held in Wisla-Jawornik from September 7-14, 1976.
44. A. J. Durelli, "The Difficult Choice," -- May 1977.  
The advantages and limitations of methods available for the analyses of displacements, strain, and stresses are considered. Comments are made on several theoretical approaches, in particular approximate methods, and attention is concentrated on experimental methods: photoelasticity, moiré, brittle and photoelastic coatings, gages, grids, holography and speckle to solve two- and three-dimensional problems in elasticity, plasticity, dynamics and anisotropy.

### Nomenclature

$a_n$	minimum diameter of ellipse or hyperbola associated with fringe order $n$
$b_n$	maximum diameter of ellipse or hyperbola associated with fringe order $n$
$E$	modulus of elasticity
$h$	distance of plate surface from neutral axis
$I(x,y)$	light intensity distribution of undeformed plate
$I'(x,y)$	light intensity distribution of deformed plate
$n$	fringe order
$p$	pitch of grating
$t$	thickness of test plate
$T(x,y)$	intensity transmittance of photographic plate recording
$T'(x,y)$	intensity transmittance of contact copy
$w(x,y)$	deformation function corrected
$x,y,z$	co-ordinates
$\epsilon_1, \epsilon_2$	maximum and minimum principal strain, respectively.
$\theta$	angle between normal to the test plate and viewing direction of camera.
$\nu$	Poisson's ratio
$\sigma_1, \sigma_2$	maximum and minimum principal stress, respectively
$\phi$	angle denoting the orientation of principal direction.

DIRECT DETERMINATION OF FLEXURAL  
STRAINS IN PLATES USING PROJECTED GRATINGS

Introduction

Plates are frequently used in engineering to resist bending loads. Depending on geometry and loading conditions, plates may be difficult to analyze mathematically. Experimental techniques are then useful. Mechanical and electrical strain gages give strains at the two faces of the plate, and from these strains moments can be computed directly. However, this information is obtained only point-by-point. Optical methods are more interesting because they give whole field information, and because no contact with the plates is required<sup>(1)</sup>. Of particular importance for this application are the projected grating,<sup>(2,3)</sup> Ligtenberg's<sup>(4)</sup> and Salet-Ikeda techniques,<sup>(5)</sup> holographic<sup>(6,7)</sup> and speckle-shearing interferometry<sup>(8)</sup>. All these optical methods measure either deflections or slope of deflections; thus it is necessary to differentiate the information once, or twice, to obtain the bending strains. These operations besides being very laborious are a source of error. The results obtained using these methods are also subjected to the limitations of the theory of plates. One of the authors used gratings directly printed on the surface of the plate and a superposed master grating to produce moiré.<sup>(9)</sup> Whole-field in-plane displacements are obtained this way and only one differentiation is required to obtain strains, but the method has not been applied yet to vibrations and is limited to relatively small deflections.

An innovative idea was introduced by Stetson<sup>(10)</sup> whereby bending moments can be determined directly using holographic interferometry. The method consists in superposing and aligning two identical transparencies of the fringe pattern of deflections obtained by holographic interferometry.

By rotating one transparency through an angle of  $180^\circ$  (in the plane of the film) with respect to the other about a point of interest, a moiré in the form of either an ellipse or a hyperbola is produced. Stetson showed that the directions and the length of the principal axes of these figures indicate the directions and the magnitude of the principal strains, respectively. Also, the relative sign of the two principal strains can be obtained from the form of the moiré pattern. An ellipse indicates that the principal strains are of the same sign. Opposite signs correspond to the hyperbola. The method permits only point-by-point analysis, but it is the only one so far developed for double differentiation.

The present paper extends the Stetson's idea to the projected grating method. While the hologram interferometry is mainly suitable for measuring very small deflections, the projected grating method can be used to determine relatively large ones. The paper includes considerations on the error inherent in the double differentiation operation and suggests how the results can be improved. A verification is also given.

#### Description of the Method

A grating is projected onto the plate (Fig. 1), in a direction making an angle  $\theta$  with the normal to the plate. The projection may be achieved by using either a projector<sup>(2)</sup> or by interference of two coherent beams<sup>(3)</sup>. When the plate is deformed, the shadow of the grating on the surface of the plate is perturbed because of the deflection. The perturbed grating is photographed by a camera viewing normally and is recorded on a photographic plate. A contact copy of the recorded grating is made on a second plate. The two plates are superposed and carefully aligned so that no moiré is seen. One of the plates is then rotated  $180^\circ$  about a point of interest. A moiré will appear in the shape of an ellipse or a hyperbola.

### Analysis

The light intensity distribution of a sinusoidal grating projected onto a flat plate can be represented by:

$$I(x,y) = 1 + \cos \frac{2\pi}{p} x \quad (1)$$

where  $I(x,y)$  is the intensity distribution;  $p$  is the grating pitch observed on the plate. The grating is running parallel to the  $y$ -axis. When the plate is deformed, the grating will be distorted accordingly and its intensity distribution becomes:

$$I'(x,y) = 1 + \cos \frac{2\pi}{p} [x - w(x,y) \cdot \tan\theta] \quad (2)$$

where  $I'(x,y)$  is the distorted grating intensity;  $\theta$  is the angle between the direction of projection and the normal to the plate, and  $w(x,y)$  is the deflection of the plate.

Assuming negative and linear recording, the intensity transmittance  $T(x,y)$  of the photographic plate recording the intensint of Eq. (2) is:

$$T(x,y) = 1 - \cos \frac{2\pi}{p} [x - w(x,y) \cdot \tan\theta] \quad (3)$$

and the intensity transmittance  $T'(s,y)$  of the contact copy is:

$$T'(x,y) = 1 + \cos \frac{2\pi}{p} [x - w(x,y) \cdot \tan\theta] \quad (4)$$

The intensity transmittance of the two transparencies superposed and aligned is represented by the product of the individual transmittances. With one plate being rotated  $180^\circ$ , and choosing the point of rotation as the origin, the resulting intensity transmittance  $T_R(x,y)$  is given by:

$$T_R(x,y) = T(x,y) \cdot T'(-x,-y) \quad (5)$$

The above equation can be expanded to yield:

$$\begin{aligned}
 T_R(x,y) = & 1 + \frac{1}{2} \cos \left\{ \frac{2\pi}{p} \tan\theta [w(x,y) + w(-x,-y)] \right\} \\
 & - \cos \frac{2\pi}{p} [x - w(x,y)\tan\theta] + \cos \frac{2\pi}{p} [-x - w(-x,-y)\tan\theta] \\
 & - \frac{1}{2} \cos \frac{2\pi}{p} [2x - w(x,y)\tan\theta + w(-x,-y)\tan\theta]
 \end{aligned} \tag{6}$$

Except for the first two terms, all the terms in the above equation are of high spatial frequency.

If the pair of plates is illuminated by a uniform intensity quasi plane wave of unity magnitude, and if one considers the average illuminance over a resolution cell  $\Delta A$ , the resulting transmitted intensity field  $I_0$  may be represented by:

$$I_0(x,y) = 1 + \frac{1}{2} \cos \left[ \frac{2\pi}{p} \tan\theta [w(x,y) + w(-x,-y)] \right] \tag{7}$$

In Eq. (7), the linear dimensions of  $\Delta A$  are considered to be large compared to the grating pitch  $p$ . Dark fringes form when

$$\frac{2\pi}{p} \tan\theta [w(x,y) + w(-x,-y)] = n\pi \tag{8}$$

where  $n = 1, 3, 5, 7, 9, \dots$ , is the fringe order.

By Taylor's series expansion about the origin and terminating at the fourth term,  $w(x,y)$  can be expressed as

$$\begin{aligned}
 w(x,y) = & w(0,0) + \left[ x \frac{\partial w(0,0)}{\partial x} + y \frac{\partial w(0,0)}{\partial y} \right] \\
 & + \frac{1}{2!} \left[ x^2 \frac{\partial^2 w(0,0)}{\partial x^2} + 2xy \frac{\partial^2 w(0,0)}{\partial x \partial y} + y^2 \frac{\partial^2 w(0,0)}{\partial y^2} \right] \\
 & + \frac{1}{3!} \left[ x^3 \frac{\partial^3 w(0,0)}{\partial x^3} + 3x^2 y \frac{\partial^3 w(0,0)}{\partial x^2 \partial y} + 3xy^2 \frac{\partial^3 w(0,0)}{\partial x \partial y^2} \right. \\
 & \left. + y^3 \frac{\partial^3 w(0,0)}{\partial y^3} \right]
 \end{aligned} \tag{9}$$

and

$$\begin{aligned}
w(-x,-y) = & w(0,0) + \left[ -x \frac{\partial w(0,0)}{\partial x} - y \frac{\partial w(0,0)}{\partial y} \right] \\
& + \frac{1}{2!} \left[ x^2 \frac{\partial^2 w(0,0)}{\partial x^2} + 2xy \frac{\partial^2 w(0,0)}{\partial x \partial y} + y^2 \frac{\partial^2 w(0,0)}{\partial y^2} \right] \\
& + \frac{1}{3!} \left[ -x^3 \frac{\partial^3 w(0,0)}{\partial x^3} - 3x^2 y \frac{\partial^3 w(0,0)}{\partial x^2 \partial y} - 3xy^2 \frac{\partial^3 w(0,0)}{\partial x \partial y^2} \right. \\
& \left. - y^3 \frac{\partial^3 w(0,0)}{\partial y^3} \right] \tag{10}
\end{aligned}$$

Define the origin such that  $w(0,0) = 0$ . If the orientation of the coordinate axes is chosen such that one of the partial derivatives of  $w(0,0)$  vanishes, then the crossed partial derivative  $\partial^2 w(0,0)/\partial x \partial y$  would vanish as well. Under these conditions,

$$w(x,y) - w(-x,-y) = x^2 \frac{\partial^2 w(0,0)}{\partial x^2} + y^2 \frac{\partial^2 w(0,0)}{\partial y^2} \tag{11}$$

and Eq. (8) can be written as

$$x^2 \frac{\partial^2 w(0,0)}{\partial x^2} + y^2 \frac{\partial^2 w(0,0)}{\partial y^2} = \frac{np}{2 \tan \theta} \tag{12}$$

The above equation represents an ellipse or a hyperbola depending on the relative signs of  $\partial^2 w(0,0)/\partial x^2$  and  $\partial^2 w(0,0)/\partial y^2$ . Since the cross derivative  $\partial w(0,0)/\partial x \partial y$  is zero,  $\partial^2 w(0,0)/\partial x^2$  and  $\partial^2 w(0,0)/\partial y^2$  measure the principal bending strains at the origin, the point about which the photographic plates is rotated. They are related to the principal diameters of the ellipse or hyperbola by:

$$\frac{\partial^2 w(0,0)}{\partial x^2} = \frac{np}{2 \tan \theta} \cdot \frac{1}{a_n^2} \tag{13}$$

$$\frac{\partial^2 w(0,0)}{\partial y^2} = \frac{np}{2 \tan \theta} \cdot \frac{1}{b_n^2} \tag{14}$$

where  $2 a_n$  and  $2 b_n$  are the principal diameters associated with fringe order  $n$ .

By measuring the principal diameters, the principal bending strain can be calculated by the following equations

$$\epsilon_1 = h \frac{\partial^2 w(0,0)}{\partial x^2} = h \frac{np}{2 \tan \theta} \cdot \frac{1}{a_n^2} \quad (15)$$

and

$$\epsilon_2 = h \frac{\partial^2 w(0,0)}{\partial y^2} = h \frac{np}{2 \tan \theta} \cdot \frac{1}{b_n^2} \quad (16)$$

where  $h$  is the distance from the neutral axis to the plate surface, and  $\epsilon_1$  and  $\epsilon_2$  are the maximum and minimum principal strains, respectively. The directions of the principal strains are indicated by the orientation of the principal diameters. To use Eqs. (15) and (16), it is necessary to obtain values of  $\frac{n}{a_n^2}$  and  $\frac{n}{b_n^2}$  as near to the point of interest as possible. Precisely at the origin, both  $n$  and  $a_n$  (or  $b_n$ ) approach zero, therefore the ratios become mathematically indeterminate.

To increase the precision of the procedure it is advisable to determine the limit of the above ratios. As one moves along a major diameter, away from the origin, values of  $\frac{1}{a_1}$ ,  $\frac{3}{a_2}$ , . . . ,  $\frac{n}{a_n}$  can be computed. A graphical extrapolation of these ratios to the origin is herein proposed as a means to estimate  $\frac{n}{a_n^2}$  as  $n$  approaches zero. This procedure was used in the next section for the experimental verification.

The above analysis is based on a sinusoidal grating. Should a square wave grating be used, the same result with better fringe visibility will be obtained. (10)

### Experimental Verification

A thin flat titanium alloy plate clamped along one side was chosen for demonstration. The plate measures 12.7 cm x 12.7 cm x 0.394 mm. Two point loads, acting in parallel but opposite direction, were applied to the test plate at locations (1) and (2) shown in Fig. 2. A grating of 16.5 lines/cm was projected onto the plate with  $\theta = 45^\circ$ . Kodak contrast process films were used for recording and copying. Figure 2 shows the test plate under loading with the grating projected on it.

In order to compare the results obtained by the proposed moiré method with the well-established electrical resistance strain gage techniques, three rectangular strain rosettes were mounted at three selected points on the plate. The exact locations of these points are shown on Fig. 2.

The pitch of the grating was first determined from a photograph of the projected grating on the undeformed test plate. The loading was then applied, and the grating on the deformed plate was photographed. Strain measurements were made before and after the photographic recording.

The experimental data obtained by the moiré method were processed in the manner as described earlier in the text. Equations (15) and (16) were employed to calculate the maximum principal strains, and  $h$  was taken to be half the thickness of the test plate.

## Results and Discussion

A summary of the experimental results is presented in Table 1. Figure 3(a) shows the elliptical moiré fringe pattern at point A on the test plate while Fig. 3(b) reveals the case of hyperbolic bending at point B. As can be observed in Table 1, the maximum principal strain and orientation of the principal direction obtained by the moiré method check well with those obtained by strain gage measurements, but the discrepancy in the case of the minimum principal strain measurements is larger. The value of the minimum strain is small and larger difference with strain gage results could be expected. The sources of error will be discussed below.

One of the major sources of error comes from the fact that the governing Eqs. (13) and (14) are based on a four term Taylor expansion of the deformation function  $w(x,y)$  and  $w(-x,-y)$  in Eqs. (9) and (10). The curvature at the center of the ellipse (or hyperbola) is determined from measurements at the extremities of the ellipse (or hyperbola). Therefore, it can be expected that the errors will grow with increase in the principal diameters. This kind of error can be reduced by increasing the density of the projected grating. Another way to improve the accuracy of the measurement is to estimate the principal strains at the center of rotation by means of the extrapolation explained earlier. Figure 4 presents a graph of principal strains for point B determined from fringe orders taken at different diameters. By means of extrapolation it is estimated that  $|\epsilon_1| = 617 \times 10^{-6}$  and  $|\epsilon_2| = 230 \times 10^{-6}$ . These results check quite well with those obtained from strain gages (see table 1).

It is assumed in the analysis of the proposed moiré method that the plate is initially flat. In fact, Eqs. (13) and (14) predict the principal

curvatures of the plate at the point of interest due to bending only. Any initial curvatures in the test plate would cause errors in the final determination.

When this proposed moiré method is used, care should be exercised in the initial alignment and subsequent rotation of the photographs. In the present experiment, this important step of data reduction was carried out on a piece of ground glass sitting on a uniform light source. The two photographic plates were aligned such that the recorded grating patterns coincided with each other. This condition was ensured by the absence of moiré fringes. When one of the photographic plates was rotated, the angle of rotation would be  $180^\circ$  when the light intensity at and near the point of rotation reached a maximum value. This condition can be ensured, for example, by employing a light meter to continuously monitor the light intensity at the point of rotation.

One major advantage of this method over the conventional strain gage technique is that the strain at any point of the plate can be determined from a single photographic record. The experimental technique is easy to apply, and unlike some other optical methods which require expensive optical equipment, this experiment can be performed with just a projector, a master grating and a camera. Although only the absolute values and the relative signs of the principal strains can be determined using this method, the actual signs of the strains at any point of the plate can be determined if the data reduction is started at a point at which the strain sign is independently known.

While holographic interferometry<sup>(10)</sup> can be used to study bending strains due to very small deformation, the proposed moiré method using a projected grating is suitable for the determination of bending strains of relatively

large magnitude. Since the quality of the photographic recording of the projected grating is inherently superior to that of the holographic fringes, the moiré pattern obtained by the projected grating method is of much better visibility, as evidenced by the results presented in Fig. 3.

#### Conclusion

A technique has been developed to determine bending strains directly using projected gratings. The method is particularly useful to study strains associated with relatively large deflections. The sensitivity of the method is proportional to the density of the projected grating and depends on the resolving capability of the imaging system.

#### Acknowledgments

The research reported in this paper has been conducted using funds partially provided by the John F. Dodge Chair, at Oakland University, and partially by the Office of Naval Research (Contract N00014-76-C-0487). Professor Durelli likes to express his appreciation for the opportunity the awarding of the Chair offers him to continue developing experimental mechanics methods and to Dr. N. Perrone, monitor of ONR, for his continuous support.

## References

1. Weller R. and Shepard B. M., "Displacement Measurement by Mechanical Interferometry," Proceedings Soc. Exp. Stress Analysis, Vol. 6, P, 1949.
2. Hovanesian J. D. and Hung Y. Y., "Moiré Contour-Sum, Contour Difference and Vibrational Analysis of Arbitrary Objects," Applied Optics, Vol. 10 (12), 1971.
3. Vest C. M. and Sweeny D. W., "Measurement of Vibrational Amplitude by Modulation of Projected Fringes," Applied Optics, Vol. 11, No. 2, 442, 1972.
4. Ligtenberg F. K., "The Moiré Method: A New Experimental Method for the Determination of Moments in Small Slab Models," Proc. SESA XII (2), 83-89, 1954.
5. Duncan J. P. and Brown C. J. E., "Slope Contours in flexed elastic plates by Salet-Ikeda technique," Proc. First Inter. Cong. Exp. Mechanics, 149-176, 1963.
6. Hovanesian J. D. and Varner J., "Methods for Determining the Bending Moments in Normally Loaded Thin Plates by Hologram Interferometry," Strathclyde Symposium on the Engineering Use of Holography, Cambridge University Press, 1968.
7. Boone P. M. and Verbiest R., "Application of Hologram Interferometry to Plate Deformation and Translation Measurement," Optica Acta, 16, 555-567, 1969.
8. Hung Y. Y. and Taylor C. E., "Measurement of Slopes of Structural Deflections by Speckle-Shearing Interferometry," Experimental Mechanics, Vol. 14, No. 7, 281-285, July 1974.

9. Durelli A. J. and Parks V. J., "Moiré Analysis of Strain," Prentice-Hall
10. Stetson K. A., "Moiré Method for Determining Bending Moments from Hologram Interferometry," Optics Technology, Vol. 2, pp. 80-84, 1970.

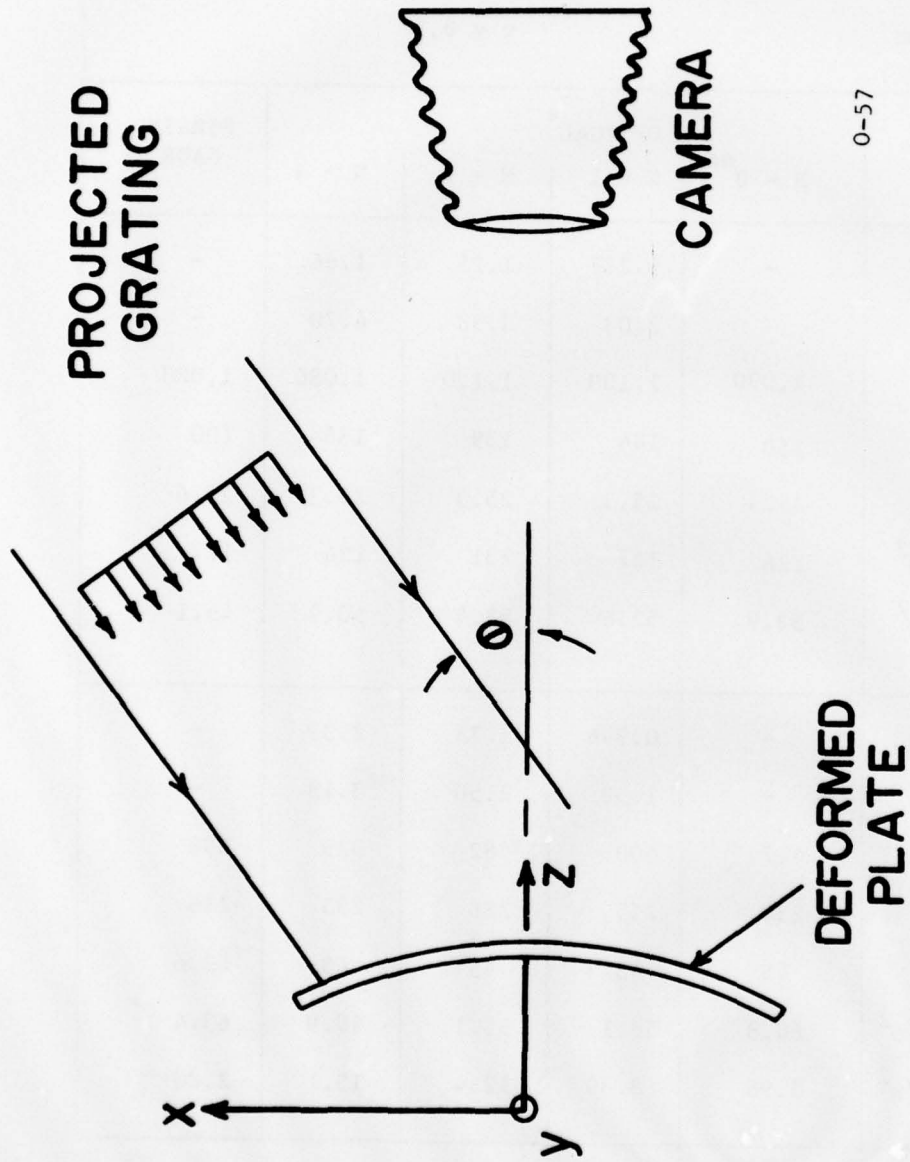
Table 1 Summary of Experimental Results

		t = 0.394 mm		tanθ = 1.02			
		h = 0.197 mm		E = 1.01 x 10 <sup>11</sup> N/m <sup>2</sup>			
		p = 0.605 mm		ν = 0.3			
LOCATION	MEASUREMENT	OPTICAL *				STRAIN GAGE	
		N = 0 **	N = 1	N = 2	N = 3		
A ***	a <sub>n</sub> , cm	-	0.737	1.25	1.66	-	
	b <sub>n</sub> , cm	-	2.03	3.58	4.70	-	
	ε <sub>1</sub> x10 <sup>6</sup>	1,090	1,100	1,120	1,080	1,020	
	ε <sub>2</sub> x10 <sup>6</sup>	150	144	139	135	100	
	φ, deg	25.3	25.3	25.3	25.3	23.6	
	σ <sub>1</sub> x10 <sup>-6</sup> , N/m <sup>2</sup>	126	127	131	124	117	
	σ <sub>2</sub> x10 <sup>-6</sup> , N/m <sup>2</sup>	52.9	52.6	53.4	50.9	45.1	
B ***	a <sub>n</sub> , cm	-	0.996	1.75	2.39	-	
	b <sub>n</sub> , cm	-	1.53	2.50	3.18	-	
	ε <sub>1</sub> x10 <sup>6</sup>	617	600	582	529	636	
	ε <sub>2</sub> x10 <sup>6</sup>	230	255	286	295	-216	
	φ, deg.	45	45	45	45	42.6	
	σ <sub>1</sub> x 10 <sup>-6</sup> , N/m <sup>2</sup>	60.8	58.1	55.1	48.9	63.4	
	σ <sub>2</sub> x 10 <sup>-6</sup> , N/m <sup>2</sup>	5.98	8.30	12.4	15.1	-2.80	

\* The proposed optical method only determines the absolute values of principal strain

\*\* Values of principal strains at n = 0 are estimated by extrapolation

\*\*\* The principal strains and stresses at location A are of the same sign, and those at location B are of the opposite sign.

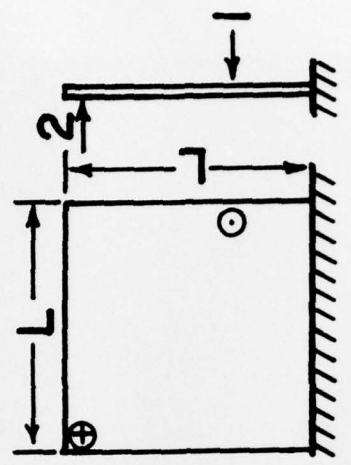


0-57

Figure 1 Experimental Set-Up of the Projected Grating Method

+ LOCATION OF  
STRAIN GAUGES

⊙, ⊕ LOCATION OF  
POINT LOAD



$P = 0.605 \text{ cm}$   
 $L = 12.7 \text{ cm}$

0-58

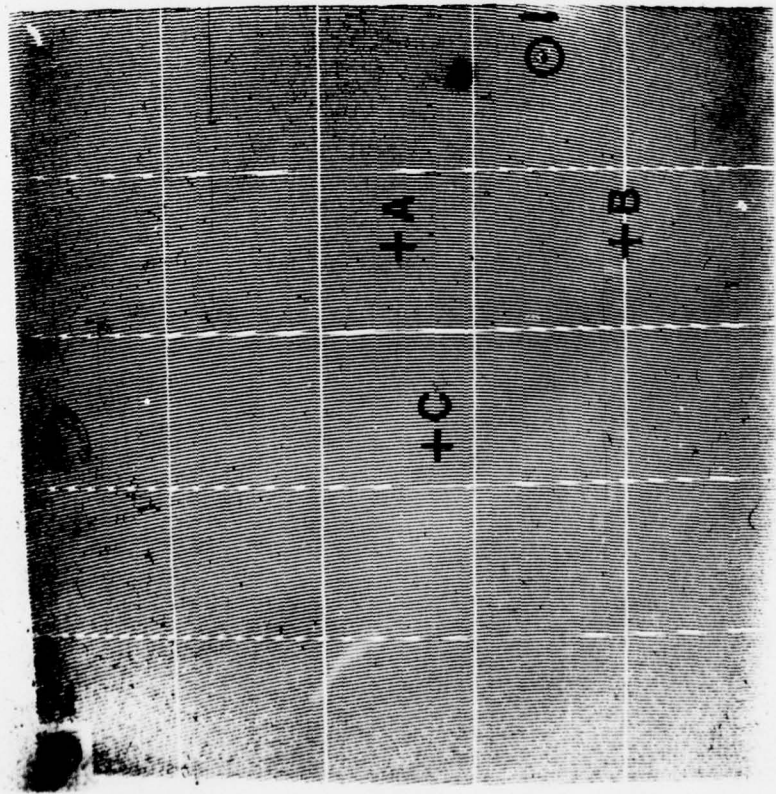
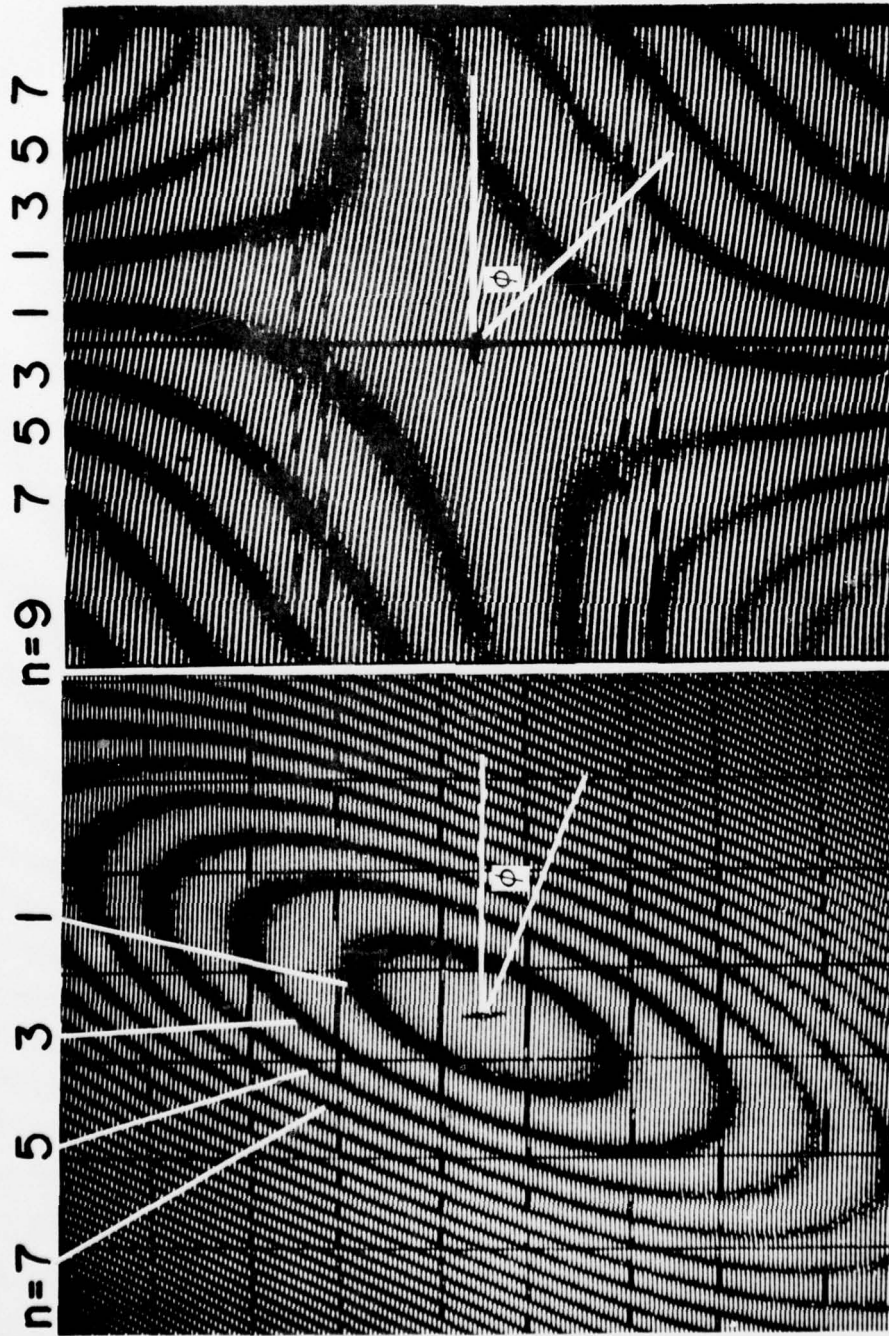


Figure 2 Grating Projected on Deformed Plate



(a) (b) 0-59

Figure 3 Moire Fringing Patterns for Double Differentiation of Out-of-Plane Deflection at (a) Point A and (b) Point B on a Plate Subjected to Twisting

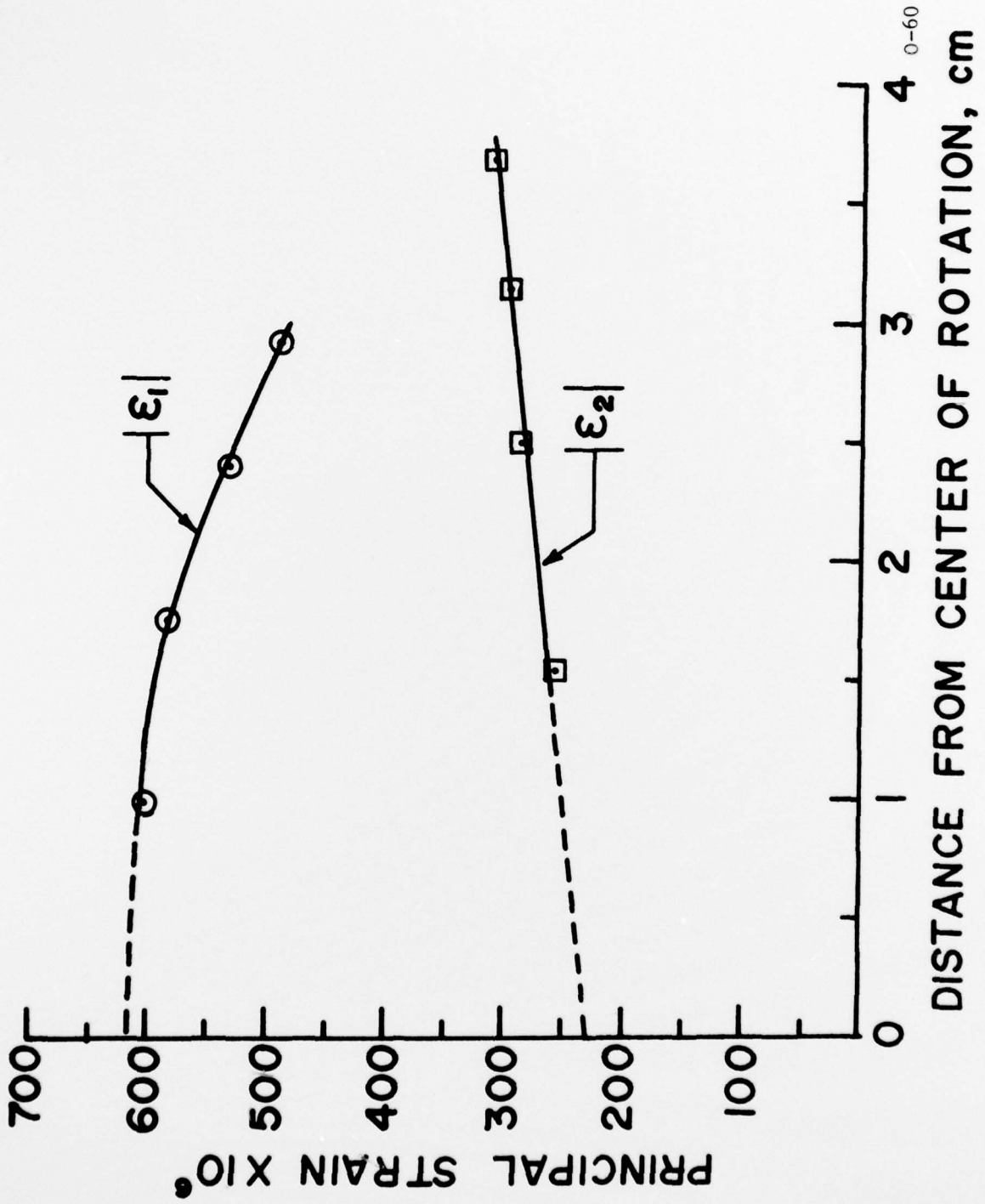


Figure 4 Principal Strain Measured at  $n = 1, 3, 5, 7$  Versus Distance from Center of Rotation at Point B on Test Plate

0-60

ONR DISTRIBUTION LIST

Part I - Government

Chief of Naval Research  
Department of the Navy  
Arlington, Virginia 22217  
Attn: Code 474 (2)  
471  
222

Director  
ONR Branch Office  
495 Summer Street  
Boston, Massachusetts 02210

Director  
ONR Branch Office  
536 S. Clark Street  
Chicago, Illinois 60604

Director  
Naval Research Laboratory  
Attn: Code 2529 (ONRL)  
Washington, D.C. 20390 (6)

U.S. Naval Research Laboratory  
Attn: Code 2627  
Washington, D.C. 20390

Commanding Officer  
ONR Branch Office  
207 West 24th Street  
New York, N.Y. 10011

Director  
ONR Branch Office  
1030 E. Green Street  
Pasadena, California 91101

Defense Documentation Center  
Cameron Station  
Alexandria, Virginia 22314 (12)

Army

Commanding Officer  
U.S. Army Research Off. Durham  
Attn: Mr. J. J. Murray  
CRD-AA-IP  
Box CM, Duke Station  
Durham, North Carolina 27706

Commanding Officer  
AMXMR-ATL  
Attn: Mr. R. Shea  
U.S. Army Materials Res. Agency  
Watertown, Massachusetts 02172

Watervliet Arsenal  
MAGGS Research Center  
Watervliet, New York 12189  
Attn: Director of Research

Redstone Scientific Info. Center  
Chief, Document Section  
U.S. Army Missile Command  
Redstone Arsenal, Alabama 35809

Army R & D Center  
Fort Belvoir, Virginia 22060

Navy

Commanding Officer & Director  
Naval Ship Res. & Dev. Center  
Bethesda, Maryland 20034  
Attn: Code 042 (Tech. Lib. Br.)  
17 (Struc. Mech. Lab.)  
172  
172  
174  
177

1800 (Appl. Math. Lab.)  
5412S (Dr. W.D. Sette)  
19 (Dr. M.M. Sevik)  
1901 (Dr. M. Strassberg)  
1945  
196 (Dr. D. Feit)  
1962

Naval Weapons Laboratory  
Dahlgren, Virginia 22448

Naval Research Laboratory  
Washington, D.C. 203  
Attn: Code 8400  
8410  
8430  
8440  
6300  
6390  
6380

Undersea Explosion Res. Div.  
Naval Ship R&D Center  
Norfolk Naval Shipyard  
Portsmouth, Virginia 23709  
Attn: Dr. E. Palmer  
Code 780

Naval Ship Res. & Dev. Center  
Annapolis Division  
Annapolis, Maryland 21402  
Attn: Code 2740 - Dr. Y. F. Wang  
28 - Mr. R.J. Wolfe  
281 - Mr. Niederberger  
2814 - Dr. H. Vanderveldt

Technical Library  
Naval Underwater Weapons Center  
Pasadena Annex  
3202 E. Foothill Blvd.  
Pasadena, California 91107

U.S. Naval Weapons Center  
China Lake, California 93557  
Attn: Code 4062 - Mr. W. Werback  
4520 - Mr. Ken Bischel

Commanding Officer  
U.S. Naval Civil Engr. Lab.  
Code L31  
Port Hueneme, California 93041

Technical Director  
U.S. Naval Ordnance Lab.  
White Oak  
Silver Spring, Maryland 20910

Technical Director  
Naval Undersea R&D Center  
San Diego, California 92132

Supervisor of Shipbuilding  
U.S. Navy  
Newport News, Virginia 23607

Technical Director  
Mare Island Naval Shipyard  
Vallejo, California 94592

U.S. Navy Underwater Sound Ref.  
Lab.

Office of Naval Research  
P.O. Box 3337  
Orlando, Florida 32806

Chief of Naval Operations  
Dept. of the Navy  
Washington, D.C. 20350  
Attn: Code Op07T

Strategic Systems Project Off.  
Department of the Navy  
Washington, D.C. 20390  
Attn: NSP- 001 Chief Scientist

Deep Submergence Systems  
Naval Ship Systems Command  
Code 39522  
Department of the Navy  
Washington, D.C. 203 60

Engineering Dept.  
U.S. Naval Academy  
Annapolis, Maryland 21402

Naval Air Systems Command  
Dept. of the Navy  
Washington, D.C. 20360  
Attn: NAVAIR 5302 Aero & Struc.  
5308 Struc.  
52031F Materials  
604 Tech. Lib.

Director, Aero Mechanics  
Naval Air Development Center  
Johnsville  
Warminster, Pennsylvania 18974

Technical Director  
U.S. Naval Undersea R&D Center  
San Diego, California 92132

Engineering Department  
U.S. Naval Academy  
Annapolis, Maryland 21402

Naval Facilities Engineering Command  
Dept. of the Navy  
Washington, D.C. 20360  
Attn: NAVFAC 03 Res. & Dev.  
04 Res. & Dev.  
14114 Tech. Lib.

Naval Sea Systems Command  
Dept. of the Navy  
Washington, D.C. 20360  
Attn: NAVSHIP 03 Res. & Tech.  
031 Ch. Scientist R&D  
03412 Hydromechanics  
037 Ship Silencing Div.  
035 Weapons Dynamics

Navy cont.

Naval Ship Engineering Center  
Prince George's Plaza  
Hyattsville, Maryland 20782  
Attn: NAVSEC 6100 Ship Sys Engr &  
Des Dep  
6102C Computer-Aided  
Ship Des  
6105G  
6110 Ship Concept Des  
6120 Hull Div.  
6120D Hull Div.  
6128 Surface Ship  
Struct.  
6129 Submarine Struct.

Air Force

Commander WADD  
Wright-Patterson Air Force Base  
Dayton, Ohio 45433  
Attn: Code WWRMDD  
AFFDL (FDDS)  
Structures Division  
AFLC (MCEEA)

Chief, Applied Mechanics Group  
U.S. Air Force Inst. of Tech.  
Wright-Patterson Air Force Base  
Dayton, Ohio 45433

Chief, Civil Engineering Branch  
WLRC, Research Division  
Air Force Weapons Laboratory  
Kirtland AFB, New Mexico 87117

Air Force Office of Scientific  
Research  
1400 Wilson Blvd.  
Arlington, Virginia 22209  
Attn: Mechanics Div.

NASA

Structures Research Division  
National Aeronautics & Space Admin.  
Langley Research Center  
Langley Station  
Hampton, Virginia 23365

National Aeronautic & Space Admin.  
Associate Administrator for Ad-  
vanced Research & Technology  
Washington, D.C. 02546

Scientific & Tech. Info. Facility  
NASA Representative (S-AK/DL)  
P.O. Box 5700  
Bethesda, Maryland 20014

Other Government Activities

Commandant  
Chief, Testing & Development Div.  
U.S. Coast Guard  
1300 E. Street, N.W.  
Washington, D.C. 20226

Technical Director  
Marine Corps Dev & Educ. Command  
Quantico, Virginia 22134

Director  
National Bureau of Standards  
Washington, D.C. 20234  
Attn: Mr. B.L. Wilson, EN 219

Dr. M. Gaus  
National Science Foundation  
Engineering Division  
Washington, D.C. 20550

Science & Tech. Division  
Library of Congress  
Washington, D.C. 20540

Director  
Defense Nuclear Agency  
Washington, D.C. 20305  
Attn: SPSS

Commander Field Command  
Defense Nuclear Agency  
Sandia Base  
Albuquerque, New Mexico 87115

Director Defense Research & Engr  
Technical Library  
Room 3C-128  
The Pentagon  
Washington, D.C. 20301

Chief, Airframe & Equipment Branch  
FS-120  
Office of Flight Standards  
Federal Aviation Agency  
Washington, D.C. 20553

Chief, Research and Development  
Maritime Administration  
Washington, D.C. 20235

Deputy Chief, Office of Ship Constr.  
Maritime Administration  
Washington, D.C. 20235  
Attn: Mr. U.L. Russo

Atomic Energy Commission  
Div. of Reactor Devel. & Tech.  
Germantown, Maryland 20767

Ship Hull Research Committee  
National Research Council  
National Academy of Sciences  
2101 Constitution Avenue  
Washington, D.C. 20418  
Attn: Mr. A.R. Lytle

Part 2 - Contractors and Other  
Technical Collaborators

Universities

Dr. J. Tinsley Oden  
University of Texas at Austin  
345 Eng. Science Bldg.  
Austin, Texas 78712

Prof. Julius Miklowitz  
California Institute of Technology  
Div. of Engineering & Applied Sci.  
Pasadena, California 91109

Dr. Harold Liebowitz, Dean  
School of Engr. & Applied Science  
George Washington University  
725 - 23rd St., N.W.  
Washington, D.C. 20006

Prof. Eli Sternberg  
California Institute of Technology  
Div. of Engr. & Applied Sciences  
Pasadena, California 91109

Prof. Paul M. Naghdi  
University of California  
Div. of Applied Mechanics  
Etcheverry Hall  
Berkeley, California 94720

Professor P.S. Symonds  
Brown University  
Division of Engineering  
Providence, R.I. 02912

Prof. A.J. Durelli  
John F. Dodge Professor  
Oakland University  
Rochester, Michigan 48063

Prof. R.B. Testa  
Columbia University  
Dept. of Civil Engineering  
S.W. Mudd Bldg.  
New York, New York 10027

Prof. H.H. Bleich  
Columbia University  
Dept. of Civil Engineering  
Amsterdam & 120th St.  
New York, New York 10027

Prof. F.L. DiMaggio  
Columbia University  
Dept. of Civil Engineering  
616 Mudd Building  
New York, New York 10027

Prof. A.M. Freudenthal  
George Washington University  
School of Engineering & Applied  
Science  
Washington, D.C. 20006

D.C. Evans  
University of Utah  
Computer Science Division  
Salt Lake City, Utah 84112

Prof. Norman Jones  
Massachusetts Inst. of Technology  
Dept. of Naval Architecture &  
Marine Engrng  
Cambridge, Massachusetts 02139

Asst. to Secretary Defense  
Atomic Energy-Att. E. Cotter  
Washington, D.C. 20301

Dr. V.R. Hodgson  
Wayne State University  
School of Medicine  
Detroit, Michigan 48202

Universities cont.

Dean B.A. Boley  
Northwestern University  
Technological Institute  
2145 Sheridan Road  
Evanston, Illinois 60201

Prof. P.G. Hodge, Jr.  
University of Minnesota  
Dept. of Aerospace Engng & Mech.  
Minneapolis, Minnesota 55455

Dr. D.C. Drucker  
University of Illinois  
Dean of Engineering  
Urbana, Illinois 61801

Prof. N.M. Newmark  
University of Illinois  
Dept. of Civil Engineering  
Urbana, Illinois 61801

Prof. E. Reissner  
University of California, San Diego  
Dept. of Applied Mechanics  
La Jolla, California 92037

Prof. William A. Nash  
University of Massachusetts  
Dept. of Mechanics & Aerospace Eng.  
Amherst, Massachusetts 01002

Library (Code 0384)  
U.S. Naval Postgraduate School  
Monterey, California 93940

Prof. Arnold Allentuch  
Newark College of Engineering  
Dept. of Mechanical Engineering  
323 High Street  
Newark, New Jersey 07102

Dr. George Herrmann  
Stanford University  
Dept. of Applied Mechanics  
Stanford, California 94305

Prof. J.D. Achenbach  
Northwestern University  
Dept. of Civil Engineering  
Evanston, Illinois 60201

Director, Applied Research Lab.  
Pennsylvania State University  
P.O. Box 30  
State College, Pennsylvania 16801

Prof. Eugen J. Skudrzyk  
Pennsylvania State University  
Applied Research Laboratory  
Dept. of Physics - P.O. Box 30  
State College, Pennsylvania 16801

Prof. J. Kempner  
Polytechnic Institute of Brooklyn  
Dept. of Aero. Engrg & Applied Mech.  
333 Jay Street  
Brooklyn, N.Y. 11201

Prof. J. Klosner  
Polytechnic Institute of Brooklyn  
Dept. of Aerospace & Appl. Mech.  
333 Jay Street  
Brooklyn, N.Y. 11201

Prof. R.A. Schapery  
Texas A&M University  
Dept. of Civil Engineering  
College Station, Texas 77840

Prof. W.D. Pilkey  
University of Virginia  
Dept. of Aerospace Engineering  
Charlottesville, Virginia 22903

Dr. H.G. Schaeffer  
University of Maryland  
Aerospace Engineering Dept.  
College Park, Maryland 20742

Prof. K.D. Willmert  
Clarkson College of Technology  
Dept. of Mechanical Engineering  
Potsdam, N.Y. 13676

Dr. J.A. Stricklin  
Texas A&M University  
Aerospace Engineering Dept.  
College Station, Texas 77843

Dr. L.A. Schmit  
University of California, LA  
School of Engineering & Applied Sci.  
Los Angeles, California 90024

Dr. H.A. Kamel  
The University of Arizona  
Aerospace & Mech. Engineering Dept.  
Tucson, Arizona 85721

Dr. B.S. Berger  
University of Maryland  
Dept. of Mechanical Engineering  
College Park, Maryland 20742

Prof. G.R. Irwin  
Dept. of Mechanical Engng.  
University of Maryland  
College Park, Maryland 20742

Dr. S.J. Fennes  
Carnegie-Mellon University  
Dept. of Civil Engineering  
Schenley Park  
Pittsburgh, Pennsylvania 15213

Dr. Ronald L. Huston  
Dept. of Engineering Analysis  
Mail Box 112  
University of Cincinnati  
Cincinnati, Ohio 45221

Prof. George Sih  
Dept. of Mechanics  
Lehigh University  
Bethlehem, Pennsylvania 18015

Prof. A.S. Kobayashi  
University of Washington  
Dept. of Mechanical Engineering  
Seattle, Washington 98105

Librarian  
Webb Institute of Naval Architecture  
Crescent Beach Road, Glen Cove  
Long Island, New York 11542

Prof. Daniel Frederick  
Virginia Polytechnic Institute  
Dept. of Engineering Mechanics  
Blacksburg, Virginia 24061

Prof. A.C. Eringen  
Dept. of Aerospace & Mech. Sciences  
Princeton University  
Princeton, New Jersey 08540

Dr. S.L. Koh  
School of Aero., Astro. & Eng. Sc.  
Purdue University  
Lafayette, Indiana 47907

Prof. E.H. Lee  
Div. of Engrg. Mechanics  
Stanford University  
Stanford, California 94305

Prof. R.D. Mindlin  
Dept. of Civil Engrg  
Columbia University  
S.W. Mudd Building  
New York, N.Y. 10027

Prof. S.B. Dong  
University of California  
Dept. of Mechanics  
Los Angeles, California 90024

Prof. Burt Paul  
University of Pennsylvania  
Towne School of Civil & Mech Engr  
Rm. 113 - Towne Building  
220 S. 33rd Street  
Philadelphia, Pennsylvania 19104

Prof. J.W. Liu  
Dept. of Chemical Engr. & Metal.  
Syracuse University  
Syracuse, N.Y. 13210

Prof. S. Bodner  
Technion R&D Foundation  
Haifa, Israel

Prof. R.J.H. Bollard  
Chairman, Aeronautical Engr. Dept.  
207 Guggenheim Hall  
University of Washington  
Seattle, Washington 98105

Prof. G.S. Heller  
Division of Engineering  
Brown University  
Providence, Rhode Island 02912

Prof. Werner Goldsmith  
Dept. of Mechanical Engineering  
Div. of Applied Mechanics  
University of California  
Berkeley, California 94720

Prof. J.R. Rice  
Division of Engineering  
Brown University  
Providence, R.I. 02912

Prof. R.S. Rivlin  
Center for the Application of  
Mathematics  
Lehigh University  
Bethlehem, Pennsylvania 18015

Bell Telephone Labs Inc.  
505 King Avenue -Tech. Lib.  
Columbus, OH 43201

Dr. Francis Cozzarelli  
Div. of Interdisciplinary  
Studies & Research  
School of Engineering  
State University of New York  
Buffalo, N.Y. 14214

Industry and Research Institutes

Library Services Dept.  
Report Section Bldg. 14-14  
Argonne National Laboratory  
9700 S. Cass Avenue  
Argonne, Illinois 60440

Dr. M.C. Junger  
Cambridge Acoustical Associates  
129 Mount Auburn St.  
Cambridge, Massachusetts 02138

Dr. L.H. Chen  
General Dynamics Corporation  
Electric Boat Division  
Groton, Connecticut 06340

Dr. J.E. Greenspon  
J.G. Engineering Research Assoc.  
3831 Menlo Drive  
Baltimore, Maryland 21215

Dr. S. Batdorf  
The Aerospace Corp.  
P.O. Box 92957  
Los Angeles, California 90009

Dr. K.C. Park  
Lockheed Palo Alto Research Lab.  
Dept. 5233, Bldg. 205  
3251 Hanover St.  
Palo Alto, CA 94304

Library  
Newport News Shipbuilding & Dry  
Dock Company  
Newport News, Virginia 23607

Dr. W.F. Bozich  
McDonnell Douglas Corporation  
5301 Bolsa Avenue  
Huntington Beach, CA 92647

Dr. H.N. Abramson  
Southwest Research Institute  
Technical Vice President  
Mechanical Sciences  
P.O. Drawer 28510  
San Antonio, Texas 78284

Dr. R.C. DeHart  
Southwest Research Institute  
Dept. of Structural Research  
P.O. Drawer 28510  
San Antonio, Texas 78284

Dr. M.L. Baron  
Weidlinger Associates, Consulting  
Engineers  
110 East 59th Street  
New York, N.Y. 10022

Dr. W.A. Von Riesmann  
Sandia Laboratories  
Sandia Base  
Albuquerque, New Mexico 87115

Dr. T.L. Geers  
Lockheed Missiles & Space Co.  
Palo Alto Research Laboratory  
3251 Hanover Street  
Palo Alto, California 94304

Dr. J.L. Tocher  
Boeing Computer Services, Inc.  
P.O. Box 24346  
Seattle, Washington 98124

Mr. William Caywood  
Code BBE, Applied Physics Laboratory  
8621 Georgia Avenue  
Silver Spring, Maryland 20034

Mr. P.C. Durup  
Lockheed-California Company  
Aeromechanics Dept., 74-43  
Burbank, California 91503

Assistant Chief for Technology  
Office of Naval Research, Code 200  
Arlington, Virginia 22217

Los Alamos Scientific Lab  
P.O. Box 1663 - Tech Labs  
Los Alamos, NM 87544

Boeing Company  
Attn. Aerospace Lab  
P.O. Box 3707  
Seattle, WA 98124

IIT Research Institute  
10 West 35th Street  
Chicago, ILL 60616



UNCLASSIFIED

SECURITY CLASSIFICATION OF THIS PAGE(When Data Entered)

permits the determination of principal strains in plates subjected to much larger deflections than the ones that can be studied using holograms. Suggestions to improve the precision of the determination are also made.

UNCLASSIFIED

SECURITY CLASSIFICATION OF THIS PAGE(When Data Entered)